REPORT DOCUMENTATION PAGE

Form Approved OMB NO. 0704-0188

1. REPORT DATE (DD-MM-YYYY)	2. REPORT TYPE	3. DATES COVERED (From - To)
02-11-2010	Final Report	1-Jan-2009 - 31-Mar-2010

4. TITLE AND SUBTITLE

Final report on Seedling project: "Suppression of Laser Shot Noise Using Laser-Cooled Opto-Mechanical Systems"

5a. CONTRACT NUMBER
W911NF-09-1-0015

5b. GRANT NUMBER

5c. PROGRAM ELEMENT NUMBER
8720AI

6. AUTHORS
Jack G. E. Harris

5d. PROJECT NUMBER

5e. TASK NUMBER

5f. WORK UNIT NUMBER

7. PERFORMING ORGANIZATION NAMES AND ADDRESSES

Yale University
Office of Sponsored Programs
Yale University
New Haven, CT 06520 -

8. PERFORMING ORGANIZATION REPORT NUMBER

9. SPONSORING/MONITORING AGENCY NAME(S) AND ADDRESS(ES)

U.S. Army Research Office
P.O. Box 12211
Research Triangle Park, NC 27709-2211

10. SPONSOR/MONITOR'S ACRONYM(S)
ARO

11. SPONSOR/MONITOR'S REPORT NUMBER(S)
55909-EL-DRP.1

12. DISTRIBUTION AVAILIBILITY STATEMENT
Approved for Public Release; Distribution Unlimited

13. SUPPLEMENTARY NOTES
The views, opinions and/or findings contained in this report are those of the author(s) and should not contrued as an official Department of the Army position, policy or decision, unless so designated by other documentation.

14. ABSTRACT

The goal of this effort was to create squeezed light with intensity fluctuations 15 dB below the shot noise level. This goal was to be achieved by integrating ultrasensitive MEMS inside a high finesse optical cavity at cryogenic temperatures. While we have not yet demonstrated squeezing, we have overcome what proved to be the most challenging technical hurdle: coupling laser light into a high finesse cavity containing an ultrasensitive MEMS at T = 5 K. Since this was the major technical novelty in this project, we expect that this device will be able to

15. SUBJECT TERMS
Optomechanics, squeezed light, cavity QED

16. SECURITY CLASSIFICATION OF:			17. LIMITATION OF ABSTRACT	15. NUMBER OF PAGES	19a. NAME OF RESPONSIBLE PERSON
a. REPORT	b. ABSTRACT	c. THIS PAGE			Jack Harris
UU	UU	UU	UU		19b. TELEPHONE NUMBER: 203-432-3826

Report Title

Final report on Seedling project: "Suppression of Laser Shot Noise Using Laser-Cooled Opto-Mechanical Systems"

ABSTRACT

The goal of this effort was to create squeezed light with intensity fluctuations 15 dB below the shot noise level. This goal was to be achieved by integrating ultrasensitive MEMS inside a high finesse optical cavity at cryogenic temperatures. While we have not yet demonstrated squeezing, we have overcome what proved to be the most challenging technical hurdle: coupling laser light into a high finesse cavity containing an ultrasensitive MEMS at T = 5 K. Since this was the major technical novelty in this project, we expect that this device will be able to demonstrate squeezing in a fairly short time.

List of papers submitted or published that acknowledge ARO support during this reporting period. List the papers, including journal references, in the following categories:

(a) Papers published in peer-reviewed journals (N/A for none)

(1) J. C. Sankey, C. Yang, B. M. Zwickl, A. E. Jayich, J. G. E. Harris, Strong and tunable nonlinear optomechanical coupling in a low-loss system, Nature Physics 6, 707 (2010).

(2) A. Nunnenkamp, K. Børkje, J. G. E. Harris, S. M. Girvin, Cooling and squeezing via quadratic optomechanical coupling, Physical Review A 82, 021806(R) (2010).

Number of Papers published in peer-reviewed journals: 2.00

(b) Papers published in non-peer-reviewed journals or in conference proceedings (N/A for none)

Number of Papers published in non peer-reviewed journals: 0.00

(c) Presentations

Number of Presentations: 0.00

Non Peer-Reviewed Conference Proceeding publications (other than abstracts):

J. C. Sankey, A. M. Jayich, B. M. Zwickl, C. Yang, J. G. E. Harris, Improved position-squared measurements using degenerate cavity modes, Proceedings of the XXI International Conference on Atomic Physics, World Scientific (Singapore) (2009).

Number of Non Peer-Reviewed Conference Proceeding publications (other than abstracts): 1

Peer-Reviewed Conference Proceeding publications (other than abstracts):

Number of Peer-Reviewed Conference Proceeding publications (other than abstracts): 0

(d) Manuscripts

Number of Manuscripts: 0.00

Patents Submitted

Patents Awarded

Graduate Students

NAME	PERCENT_SUPPORTED
Andrew Jayich	0.50
Cheng Yang	0.42
Ben Zwickl	0.25
FTE Equivalent:	**1.17**
Total Number:	**3**

Names of Post Doctorates

NAME	PERCENT_SUPPORTED
Jack Sankey	0.50
FTE Equivalent:	**0.50**
Total Number:	**1**

Names of Faculty Supported

NAME	PERCENT_SUPPORTED
FTE Equivalent:	
Total Number:	

Names of Under Graduate students supported

NAME	PERCENT_SUPPORTED
FTE Equivalent:	
Total Number:	

Student Metrics

This section only applies to graduating undergraduates supported by this agreement in this reporting period

The number of undergraduates funded by this agreement who graduated during this period:	0.00
The number of undergraduates funded by this agreement who graduated during this period with a degree in science, mathematics, engineering, or technology fields:.....	0.00
The number of undergraduates funded by your agreement who graduated during this period and will continue to pursue a graduate or Ph.D. degree in science, mathematics, engineering, or technology fields:.....	0.00
Number of graduating undergraduates who achieved a 3.5 GPA to 4.0 (4.0 max scale):	0.00
Number of graduating undergraduates funded by a DoD funded Center of Excellence grant for Education, Research and Engineering:	0.00
The number of undergraduates funded by your agreement who graduated during this period and intend to work for the Department of Defense	0.00
The number of undergraduates funded by your agreement who graduated during this period and will receive scholarships or fellowships for further studies in science, mathematics, engineering or technology fields:	0.00

Names of Personnel receiving masters degrees

NAME
Total Number:

Names of personnel receiving PHDs

NAME

Total Number:

Names of other research staff

NAME PERCENT_SUPPORTED

FTE Equivalent:

Total Number:

Sub Contractors (DD882)

Inventions (DD882)

Final Report on Seedling Project "Suppression of Laser Shot Noise Using Laser-Cooled Optomechanical Systems" (Contract #: W911NF-09-1-0015) April 22, 2010

Jack Harris, *Department of Physics, Yale University, New Haven, CT.*

Executive Summary: The goal of this effort was to create squeezed light with intensity fluctuations 15 dB below the shot noise level. This goal was to be achieved by integrating ultrasensitive MEMS inside a high finesse optical cavity at cryogenic temperatures. While we have not yet demonstrated squeezing, we have overcome what proved to be the most challenging technical hurdle: coupling laser light into a high-finesse cavity containing an ultrasensitive MEMS at T = 5 K. Since this was the major technical novelty in this project, we expect that this device will be able to demonstrate squeezing in a fairly short time.

Background: The goal of this effort was to create laser light with intensity fluctuations below the shot noise level. This type of light (known as "squeezed" light) can improve the performance of optical instruments which are presently limited by photon shot noise. Specific theoretical proposals have considered applications for squeezed light in laser gyroscopes, trace gas detectors, interferometers, and magnetometers.

To date, squeezed light has been produced only in proof-of-principle experiments, and has not yet been applied to any instruments. The present world record for shot noise suppression is 10 dB, but achieving this typically requires a full optical table of equipment and constant fine tuning. The principle challenge in producing squeezed light has been meeting two simultaneous requirements in a single device: strong optical nonlinearity (to alter the photon statistics) and low optical absorption (to avoid adding quantum noise to the laser beam). In most nonlinear optical materials these two quantities are not independent, and typically one must strike a compromise between them.

The goal of our work has been to use a novel form of optical nonlinearity to circumvent this compromise and produce strongly squeezed light (15 dB suppression of shot noise). Specifically, we have developed an ultrasensitive MEMS device which is coupled via radiation pressure to an optical cavity. This optomechanical device is expected to achieve optical nonlinearity because photons in the cavity displace the membrane (via radiation pressure), and the displacement of the membrane in turn detunes the cavity.

The resulting intensity-dependent cavity detuning is equivalent to a Kerr-type nonlinearity. However this optomechanical device's nonlinearity is achieved without passing the light through a solid medium. As a result, its optical absorption can be much lower than in traditional nonlinear devices. This allows the cavity finesse to be increased, leading to stronger optical nonlinearity.

The squeezing performance of such a device has been calculated analytically. These calculations indicate that the device's performance is optimized when the cavity finesse F is high, the membrane's mechanical quality factor Q is high, and the membrane's Brownian motion is small.

Accomplishments During This Seedling Project: To meet these technical requirements, we began this seedling project by designing and constructing a high-finesse

optical cavity that incorporates a micromechanical membrane and is capable of operating inside a cryostat.

Figure 1 shows the basic schematic of the apparatus. The cavity is assembled at room temperature and laser light is coupled into the cavity using free space optics. Upon cooling from room temperature to the cryostat's base temperature, thermal contractions inevitably cause the cavity to become misaligned. Provided this misalignment is small, it can be compensated for by adjusting the room temperature optics on the top of the cryostat. The membrane's alignment to the cavity axis must also be maintained during the cool down. This is accomplished through the use of *in situ* cryogenic translation stages.

Since the operation of a high-finesse cavity inside a cryostat is a highly non-standard requirement, at the start of this project (January 2009 – March 2009) we conducted several incremental tests of this apparatus' performance. First we used our cryostat to cool a high-finesse cavity without a micromechanical membrane. The purpose of this was to test whether we could use free space optics to maintain coupling to the optical cavity while it cooled. This test was successful; thermal contractions inside the cryostat could be compensated for using the room temperature optics. Figure 2A shows measurements of this "empty" cavity's ringdown at T = 4 K. The cavity finesse determined from this data is in good agreement with the value measured at room temperature, indicating that the cavity mirrors are essentially unaffected by operation at low temperatures. Similar results were achieved with the fridge at T = 0.4 K, and we were able to determine that laser powers up to 0.1 mW did not heat the fridge by more than a few mK.

The second incremental test we performed was to measure the membrane's optical absorption. For simplicity, these measurements were performed at room temperature. Our previous work had used non-stochiometric SiN_x membranes whose absorption corresponded to an imaginary index of refraction $\mathrm{Im}(n) = 2\times10^{-4}$ (this data is shown on the left-hand side of Figure 2B). This absorption, while fairly low, meant that if the membrane was placed anywhere but at a node if the intracavity standing wave, the need to avoid heating the membrane via optical absorption limited the useable cavity finesse to ~10,000.

We had been told by colleagues at Caltech (O. Painter, C. Regal) that stochiometric Si_3N_4 membranes might have much lower absorption, so during this seedling project we repeated these measurements with a stochiometric membrane, producing the results on the right-hand side of Figure 2B. The cavity's finesse is modulated by only a few percent as the membrane is moved from node to antinode, but since this modulation is not sinusoidal, it does not appear to be due to absorption in the membrane (which should be proportional to the overlap between the optical standing wave and the membrane). The observed modulation of the cavity finesse is believed to be due to the scattering of light between different transverse modes. Although such scattering can limit the usable finesse, it does not result in heating of the membrane. Based on the data in Figure 2B we estimate that $\mathrm{Im}(n) < 2\times10^{-4}$ in these stochiometric membranes. These stochiometric membranes achieve the same high mechanical quality factor ($Q = 1\times10^6$) as the nonstochiometric membranes. These results are incorporated in a paper which has just been accepted for publication in *Nature Physics* (currently available as ArXiv:1002.4158).

With these preliminary tests conducted, we proceeded to design and build the actual device (April 2009 – May 2009). The cryogenic cavity demonstrated in Figure 2A was modified to include a membrane, as well as cryogenic translation stages for aligning the membrane within the cavity. The final apparatus is shown in Figure 3, which gives both an external view of the room temperature optics and an internal view of the device itself.

In cooling down the modified cavity (which now incorporated the membrane) we found that thermal contractions (or other effects) left the cavity too misaligned to be corrected using the room temperature optics. This does not require a very large misalignment – once the cavity axis has shifted enough that it no longer points out the 1 cm diameter, 2 m long clear shot tube, it is no longer possible for the room temperature optics to couple a laser beam to the cavity.

The period June 2009 – March 2010 was spent debugging this problem. The solution involved a careful redesign of the cryogenic optical setup to minimize asymmetry, strains, and dissimilar materials. In early March, we were able to cool down our device while maintaining full optical coupling to the cavity and full control over the membrane's position inside the cavity.

Figure 4 shows a measurement of the cavity's optical ringdown (taken at T = 5 K) with the membrane at a node of the cavity mode (upper panel) and at an antinode (lower panel). As expected, the measured cavity finesse varies by ~1%, indicating that the membrane is not absorbing an appreciable amount of the intracavity light.

Figure 5 shows a measurement of the membrane's mechanical resonance near 523 kHz. The mechanical *Q* factor appears low because this data was taken with helium exchange gas inside the fridge's vacuum space. We have since removed the exchange gas and have begun characterizing the membrane in vacuum.

The most recent data we have taken is shown in Figure 6, which plots the fluctuations in the intensity of a laser beam reflecting off of the cryogenic optomechanical device described above. The goal of this project was to have the fluctuations of this beam suppressed below the shot noise level. As described above, we have not yet achieved this (mostly owing to the delay in debugging the cryogenic operation of the experiment), but with the apparatus working in the last month, we are rapidly approaching this goal.

In Figure 6, the black curve (lowermost) is the detector noise measured in the absence of a laser beam. The dashed curve (just above the detector noise) is the expected shot noise for the laser power used in the remaining data traces. As can be seen, it is above the detector noise and so should be observable. The blue trace in Figure 6 corresponds to a laser beam which is deliberately detuned from the cavity resonance, and so is simply reflected from the front mirror of the cavity without interacting with either the cavity or the membrane. This serves a baseline measurement of our laser noise. As can be seen, it is roughly an order of magnitude above the expected shot noise. Presumably this represents technical noise in our laser; in future measurements this will be passively filtered using a reference cavity, which is already assembled and tested in our lab.

The green, gray, and red traces correspond to data taken with the laser locked to the cavity resonance (and so interacting with the cavity and the membrane). In the gray trace, the membrane is positioned at a node of the intracavity field; as a result, we expect it to interact minimally with the laser beam and so to produce very little optomechanical

effect. In the green and red traces the membrane is displaced slightly from the node, into a region where the optical standing wave overlaps more strongly with the membrane. At present we have not observed any impact of the membrane's motion on the laser noise, but we are presently working on this. One important issue is that the data in Figure 6 was taken with the laser tuned precisely to the cavity resonance, whereas the strongest optomechanical effects are expected when the laser is detuned by roughly one linewidth.

It should be possible to modify the laser detuning and membrane position in situ with the present set up. Once this is accomplished and other minor technical issues are debugged, we expect to see the membrane's response suppress the laser noise. We expect that this will require a few more months, and that the single greatest technical challenge (maintaining optical coupling to the cryogenic cavity) has been overcome during the period of this seedling.

We note that in parallel with these experimental efforts we have collaborated with theory colleagues at Yale (Steven Girvin and his group) to consider the possibilities for generating squeezed light via different types of optomechanical coupling. We have developed a theory for the squeezing produced by a quadratic optomechanical coupling, which our devices are capable of realizing (in addition to the usual linear coupling). This work has been submitted to Physical Review Letters.

Publications Resulting From This Work:

- Nunnenkamp, K. Børkje, J. G. E. Harris, S. M. Girvin, *Cooling and squeezing via quadratic optomechanical coupling*, ArXiv:1004.2510 (submitted to Physical Review Letters, 2010).

- J. C. Sankey, C. Yang, B. M. Zwickl, A. E. Jayich, J. G. E. Harris, *Strong and tunable nonlinear optomechanical coupling in a low-loss system*, ArXiv:1002.4158 (submitted to Nature Physics, 2010).

Copies of each of these papers are attached to this report.

Final Report on Seedling Project "Suppression of Laser Shot Noise Using Laser-Cooled Optomechanical Systems"
(Contract #: W911NF-09-1-0015)
April 22, 2010
Jack Harris, *Department of Physics, Yale University, New Haven, CT.*

FIGURE 1: Schematic of a cryogenic high-finesse cavity with an integrated micromechanical membrane. Laser light is coupled into the cavity from room temperature via free space optics.

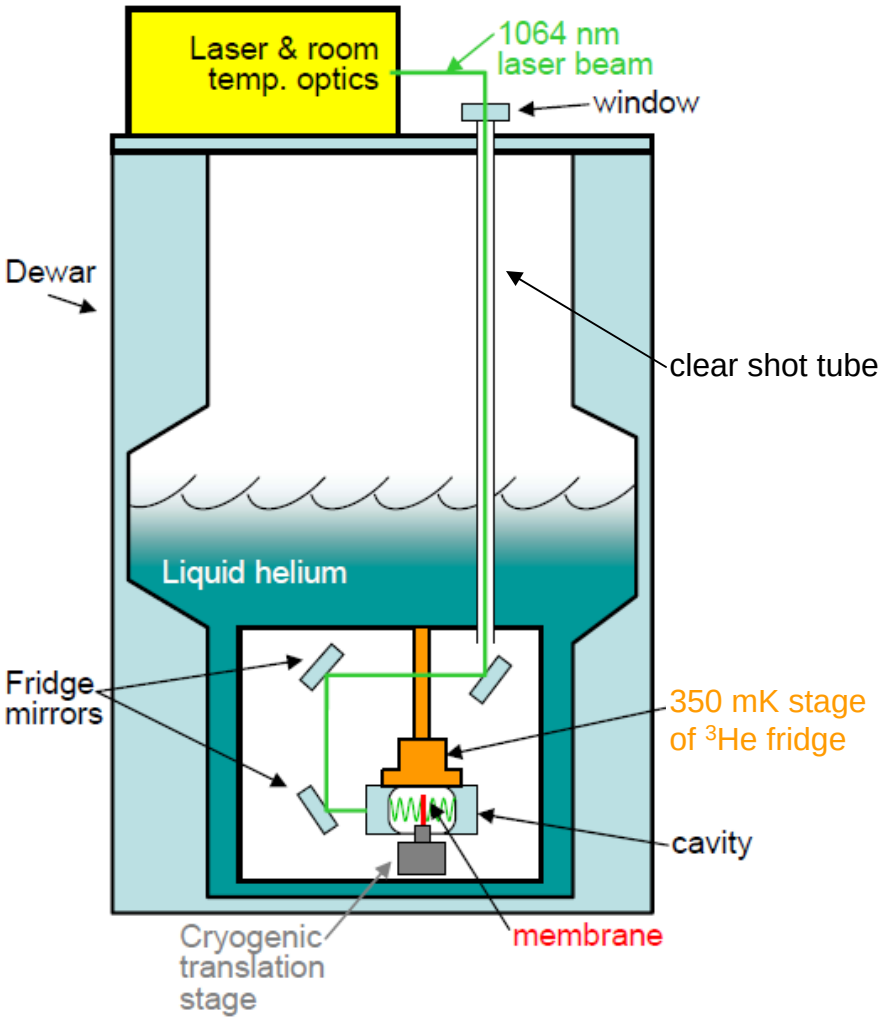

FIGURE 2: Preliminary characterization

Figure 2A: Optical ringdown of an empty cavity (i.e., without a membrane) inside our cryostat at T = 4K. The fit is to a single exponential and returns a value for the finesse of 71,000, equivalent to the value measured at room temperature.

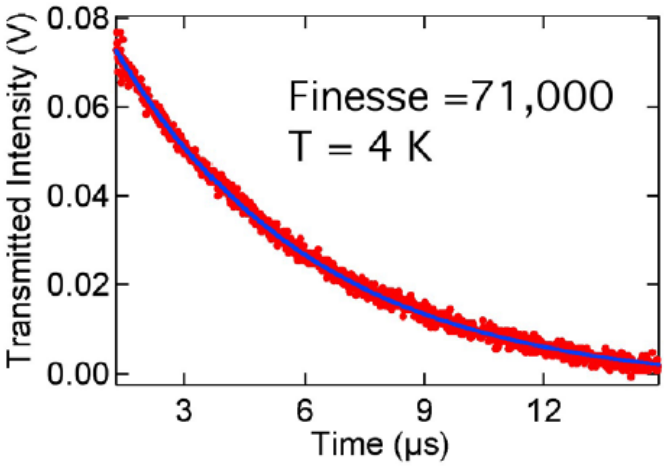

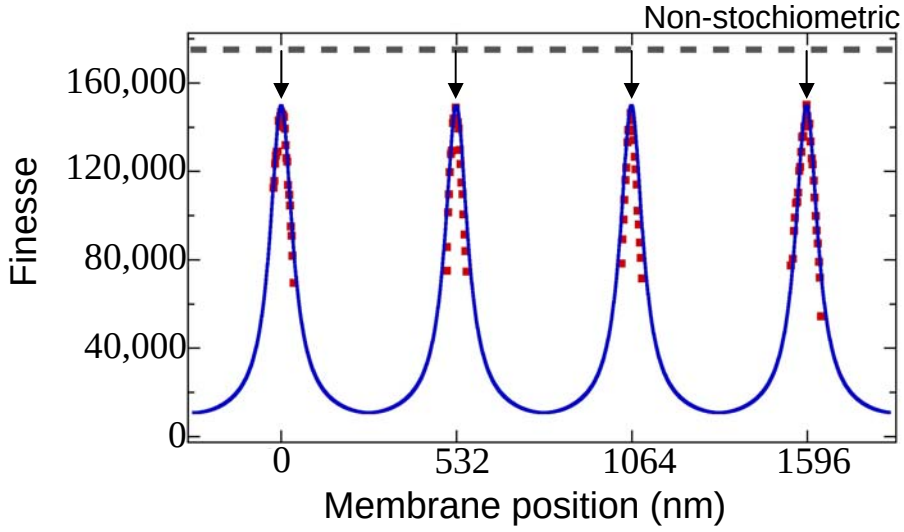

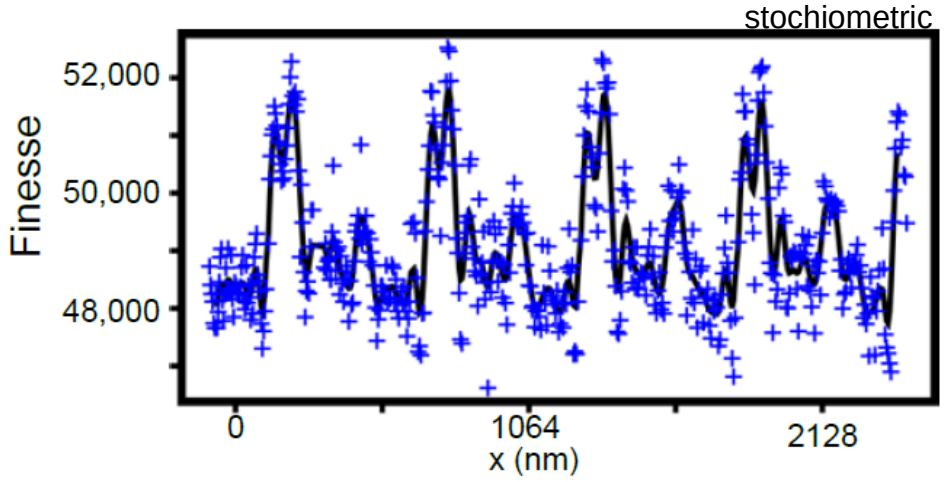

Figure 2b: Comparison of absorption for a nonstochiometric membrane (left panel) and a stochiometric membrane (left panel). The nonstochiometric membrane absorbs strongly whenever it is away from a node of the intracavity standing wave (arrows), resulting in a strong decrease of the cavity finesse. The dashed line shows the cavity finesse when the membrane is removed. The solid line is a fit to the data and gives Im(n) = 2 $\times 10^{-4}$. Stochiometric membranes, by contrast, absorb very little light (right panel). For this measurement the empty cavity finesse was 50,000. The small modulations in the finesse reflect scattering between transverse modes, not absorption.

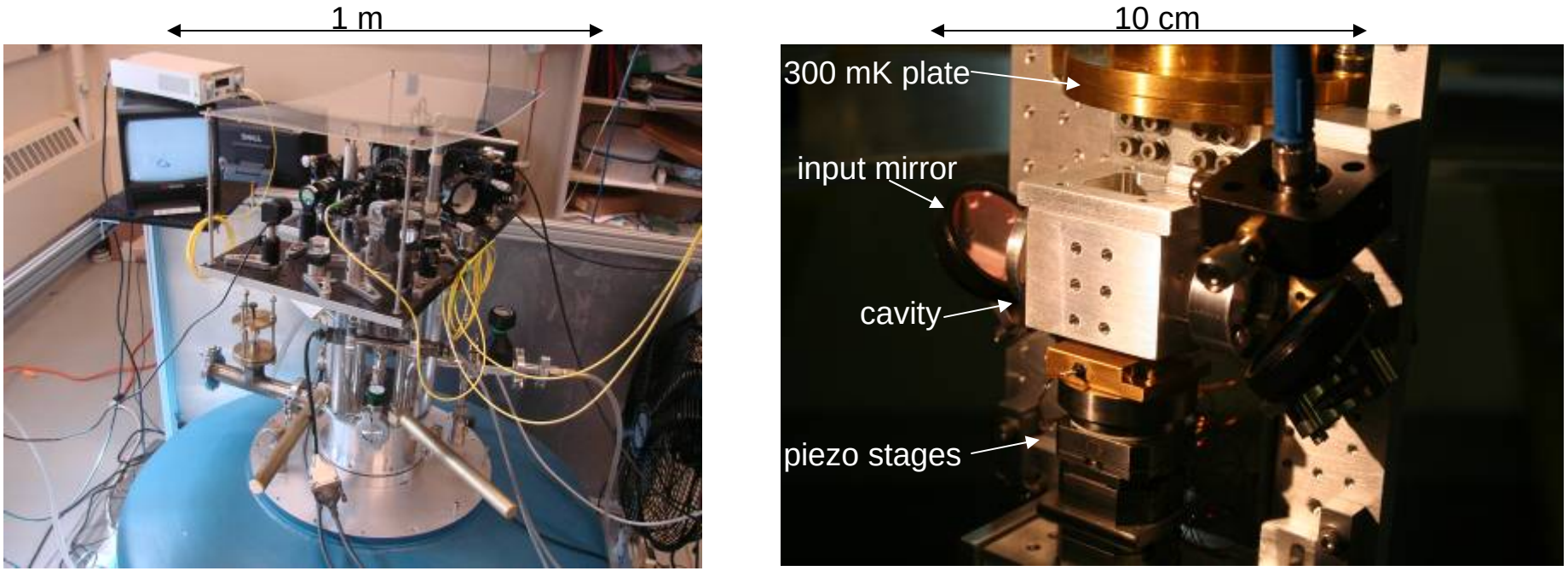

Figure 3: The experimental cryostat. Left: photograph of the exterior of the cryostat (blue). An optical breadboard (black) is mounted to the top of the cryostat, allowing laser light to be aligned down the cryostat's clear-shot tubes. The laser light is delivered to the cryostat via optical fibers (yellow). Right: photograph of the interior of the cryostat, showing the ^{3}He cold plate (gold), the cavity, and the piezoelectric translation stages which allow the membrane to be positioned within the cavity *in situ*.

Figure 4: Optical ringdown of the cavity containing a membrane at T = 5 K. Upper panel: ringdown with the membrane at a node of the optical standing wave. The red curve is a fit to a single exponential giving a cavity finesse 80,000. Lower panel: ringdown with the membrane at an antinode of the optical standing wave. The red curve is a fit to a single exponential giving a cavity finesse 80,000.

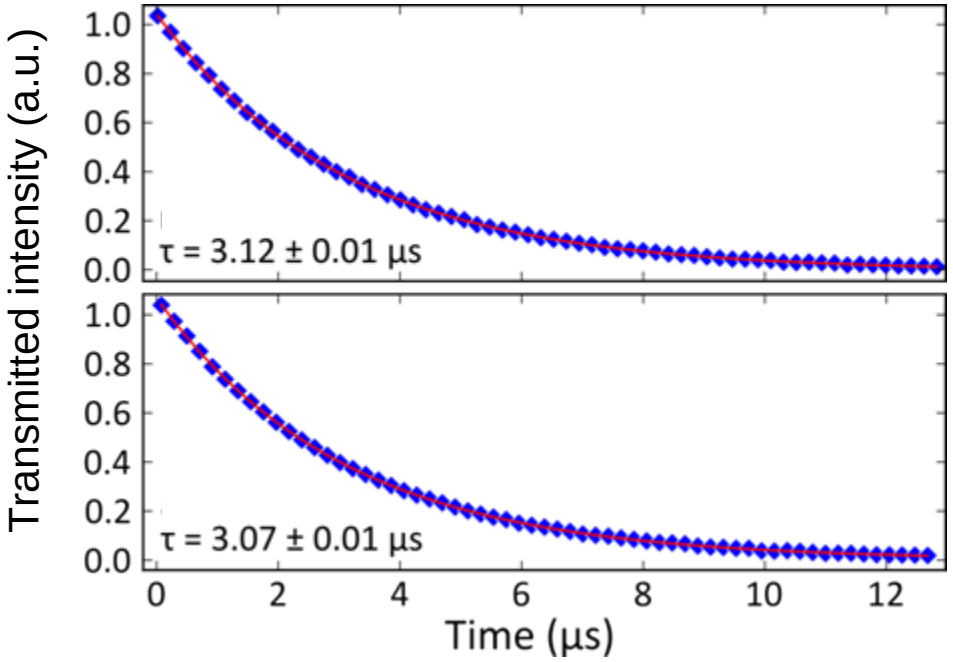

Figure 5: Measurement of the mechanical resonance of the membrane inside the cavity at T = 5 K. The low quality factor is due to the fact that this data was taken with helium exchange gas inside the fridge.

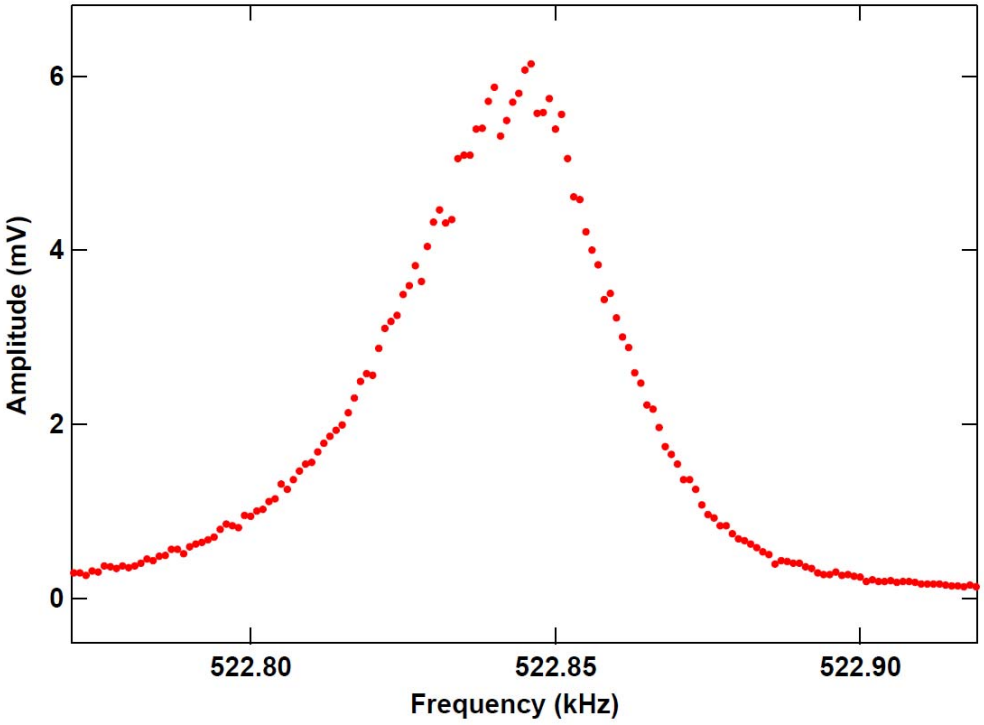

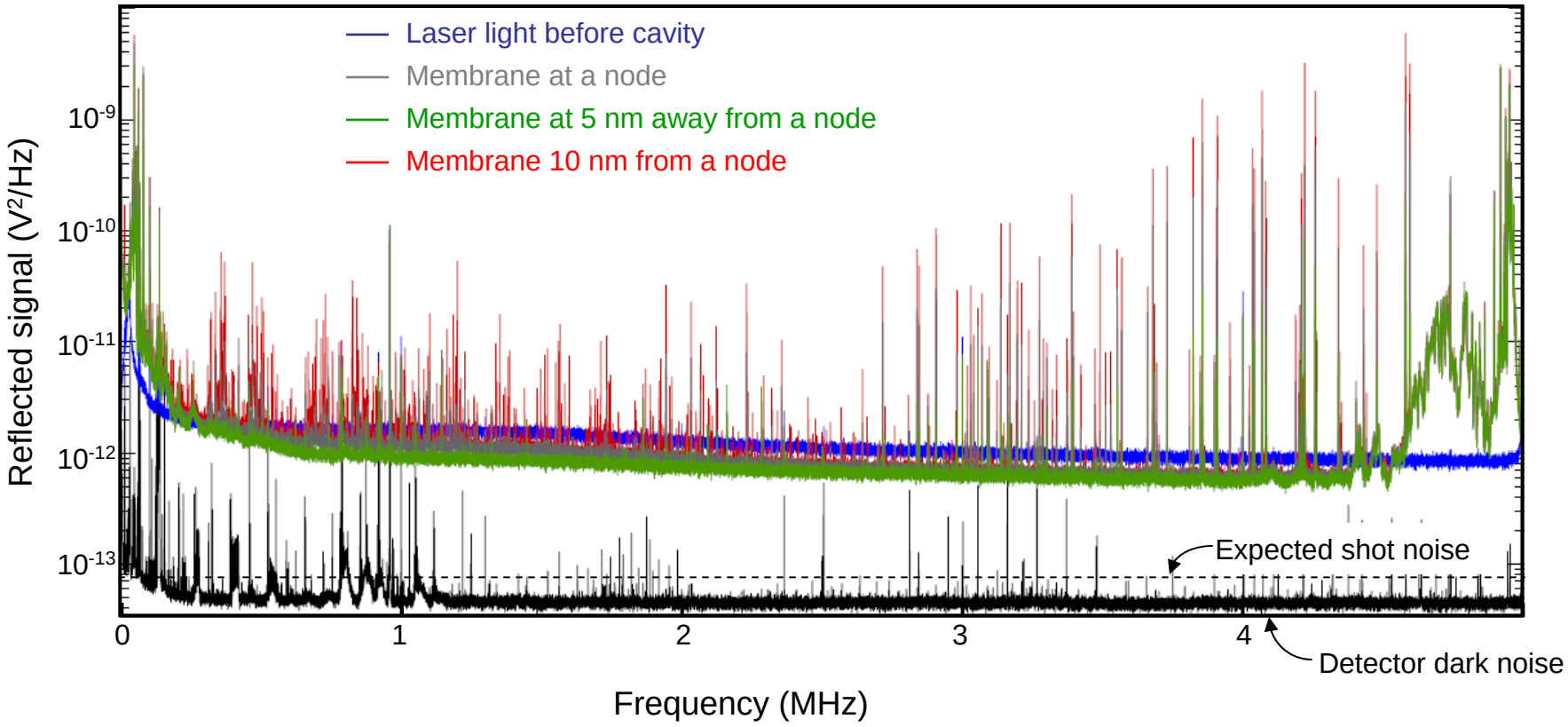

Figure 6: Preliminary measurement of laser noise reflected from a cryogenic (T = 5 K) optomechanical cavity. The expected shot noise (dashed line) is well above the detector dark noise (black). However it is at present obscured by technical noise from the laser (blue). Tuning the laser onto resonance with the optomechanical cavity (gray, green, and red) produces small changes in the observed noise, but substantial optimization of the input laser noise as well as laser power and detuning relative to the cavity remains to be done in the near term.

Strong and Tunable Nonlinear Optomechanical Coupling in a Low-Loss System

J. C. Sankey[1], C. Yang[1], B. M. Zwickl[1], A. M. Jayich[1], J. G. E. Harris[1,2,*]

[1] Department of Physics, Yale University, New Haven, CT 06520, USA

[2] Department of Applied Physics, Yale University, New Haven, CT 06520, USA

*e-mail jack.harris@yale.edu

April 21, 2010

Abstract

A major goal in optomechanics is to observe and control quantum behavior in a system consisting of a mechanical resonator coupled to an optical cavity. Work towards this goal has focused on increasing the strength of the coupling between the mechanical and optical degrees of freedom; however, the form of this coupling is crucial in determining which phenomena can be observed in such a system. Here we demonstrate that avoided crossings in the spectrum of an optical cavity containing a flexible dielectric membrane allow us to realize several different forms of the optomechanical coupling. These include cavity detunings that are (to lowest order) linear, quadratic, or quartic in the membrane's displacement, and a cavity finesse that is linear in (or independent of) the membrane's displacement. All these couplings are realized in a single device with extremely low optical loss and can be tuned over a wide range *in situ*; in particular, we find that the quadratic coupling can be increased three orders of magnitude beyond previous devices. As a result of these advances, the device presented here should be capable of demonstrating the quantization of the membrane's mechanical energy.

Nearly all optomechanical systems realized to date can be characterized by a linear relationship

between the optical cavity's detuning $\omega(x)$ and the displacement of the mechanical element x.[1] In the classical regime this "linear" optomechanical coupling has enabled powerful laser cooling and sensitive displacement readout of the mechanical element.[2–7] As $\omega' \equiv \partial\omega/\partial x$ increases this linear coupling becomes stronger, and it should become possible to observe quantum effects such as laser-cooling to the mechanical ground state,[8,9] quantum-limited measurements of force and displacement,[10,11] and the production of squeezed light.[12] In the quantum regime, however, the *form* of the optomechanical coupling plays a crucial role in determining which phenomena are observable. For example, linear coupling provides a continuous readout of x, and so precludes a direct measurement of one of the most striking features associated with the quantum regime: the quantization of the mechanical oscillator's energy.

One device that has demonstrated a nonlinear optomechanical coupling consists of a thin dielectric membrane placed inside a Fabry-Perot cavity.[13] With the membrane positioned at a node (or antinode) of the intracavity standing wave, $\omega(x) \propto x^2$ to lowest order. This "quadratic" optomechanical coupling is compatible with a quantum nondemolition (QND) readout of the membrane's energy $H_m = \hbar\omega_m n_m$, where ω_m is the membrane's resonant frequency and n_m is the membrane's phonon number. Two distinct schemes have been proposed for using this quadratic coupling to demonstrate the quantization of the membrane's energy. Both schemes assume the membrane is laser-cooled to mean phonon number $\langle n_m \rangle < 1$. Numerical estimates indicate this level of cooling should be feasible for the device described here, provided it is pre-cooled cryogenically.[8,9]

The goal of the first scheme is to monitor n_m with resolution sufficient to observe individual quantum jumps. This is not feasible with the devices demonstrated to date, and would require substantial improvements to the quadratic coupling strength $\omega'' \equiv \partial^2\omega/\partial x^2$, the membrane's optical absorption, and the membrane's mechanical properties.[13]

In the second scheme, the laser-cooled membrane would be mechanically driven from the ground state to a large-amplitude coherent state with $\langle n_m \rangle \gg 1$. The quadratic coupling would then be used to monitor the membrane's energy with resolution sufficient to resolve fluctuations $\propto \sqrt{\langle n_m \rangle}$

corresponding to the shot noise of the membrane's phonons. Detailed calculations[14] show that this second scheme is considerably less demanding than the first, though it still requires substantial improvements to ω'' and the membrane's optical absorption.

Here we demonstrate an optomechanical device in which ω'' is increased by at least three orders of magnitude, while the membrane's optical absorption is substantially decreased. The device satisfies the requirements for observing phonon shot noise at a bath temperature $T = 300$ mK, and represents substantial progress toward observing individual quantum jumps. The improvement in ω'' is achieved by exploiting the full spectrum of the optical cavity's transverse modes, which exhibits numerous avoided crossings as a function of the membrane's position. These crossings were not considered in previous work, which assumed a one-dimensional model of the cavity and only a single transverse optical mode.[13,15]

In addition to increased ω'', we demonstrate considerable flexibility within a single device: (i) ω'' can be varied *in situ* by adjusting the position and tilt of the membrane; (ii) it is possible to tune ω'' to zero, thereby realizing a purely quartic optomechanical coupling $\omega(x) \propto x^4$; (iii) the gradient of the cavity relaxation $\kappa' \equiv \partial\kappa/\partial x$ can be tuned over a wide range or set to zero; and (iv) cavity modes with different forms of $\omega(x)$ (e.g., linear and quadratic) can be simultaneously addressed using multiple laser frequencies, allowing for simultaneous laser cooling and QND energy readout. Each type of coupling offers distinct functionality, and together they represent a new set of tools for observing and controlling quantum effects in optomechanical systems. We find that the features in the cavity spectrum responsible for these couplings are reproduced by a straightforward theoretical model, allowing for optimization of future devices.

1 Strong purely-quadratic optomechanical coupling

Our optomechanical system is shown schematically in Fig. 1a. Two fixed end mirrors (radius of curvature $R = 5$ cm) form a Fabry-Perot cavity with free spectral range 2.374 GHz (length

$L = 6.313$ cm) and empty-cavity finesse $F = 50,000$. A 1-mm-square flexible Si_3N_4 membrane of nominal thickness $t = 50$ nm and real refractive index $\mathrm{Re}[n] = 2.0$ is placed near the cavity waist. The membrane is mounted on a motorized stage, providing control over the membrane's coarse position along the cavity axis ($\tilde{x}$) as well as its tilt about the two transverse axes ($\tilde{y}$ and $\tilde{z}$). Piezoelectric transducers allow for nanometer-scale displacements along $\tilde{x}$.

Figure 1b shows the cavity's transmission spectrum as a function of membrane position x. The cosine-like detuning curves are similar to those demonstrated previously,[13] and achieve $\omega''/2\pi = 30$ kHz/nm^2 at their extrema. The data in Fig. 1b were taken with the laser coupled to several of the cavity's lower-order transverse modes, and a number of apparent crossings between these modes can be seen. We focus specifically on the region highlighted by the dotted box in Fig. 1b, where the TEM_{00} "singlet" and the $\mathrm{TEM}_{\{20,11,02\}}$ "triplet" modes cross. Figure 1c shows this region in greater detail with the membrane (i) lying in the $\tilde{y}$-$\tilde{z}$ plane and (ii) tilted by 0.4 mrad about the $\tilde{z}$-axis. The behavior in Fig. 1c(ii) is ubiquitous among multiplets of higher-order transverse modes: tilting the membrane lifts the multiplet degeneracy, with modes of greater spatial extent along the membrane slope ($\tilde{y}$ in this case) perturbed the most.

The central result of this article is illustrated in Fig. 1d, which shows a high-resolution scan of the region indicated by the dotted box in Fig. 1c. This data demonstrates that the apparent crossings between the various optical modes are avoided, and that at their anticrossings $\omega(x)$ is purely quadratic with $\omega''/2\pi$ substantially greater than 30 kHz/nm^2. For example, the TEM_{20} - TEM_{00} crossing in Fig. 1d shows $\omega''/2\pi = 4.5$ MHz/nm^2 (dashed white lines). The TEM_{02} - TEM_{00} crossing is not resolved in the main body of Fig. 1d, but the line-scan in the inset shows a splitting ≈ 200 kHz between these modes. Assuming the crossing is of the usual hyperbolic form $\omega(x) = \pm\sqrt{(\omega' x)^2 + \omega_s^2}$, where ω' is the slope of $\omega(x)$ far from the crossing and $2\omega_s$ is the gap at the degeneracy point, the data in the inset indicate $\omega''/2\pi \gtrsim 30$ MHz/nm^2, which is three orders of magnitude greater than previously demonstrated.[13]

We note that if the membrane is positioned so that two modes realize a quadratic coupling,

other modes will still realize a linear coupling. In Fig. 1d this occurs at the position $x = 0$ nm: here the eigenmodes formed by the TEM_{02} and TEM_{00} modes exhibit quadratic coupling while the TEM_{11} mode's coupling is linear. This means that lasers tuned to different eigenmodes can simultaneously exploit different forms of the optomechanical coupling.

We can understand the origin of these features by noting that avoided crossings generally reflect a broken symmetry that prevents eigenmodes from becoming degenerate. An ideal empty Fabry-Perot cavity possesses symmetry that allows degeneracy between transverse modes, but in our device we expect this symmetry to be broken for two reasons: the curved wavefronts of the cavity modes may not overlap perfectly with the flat membrane (e.g., if the membrane is tilted or displaced from the cavity waist), and the empty cavity itself may be slightly asymmetric (e.g., owing to imperfect form of the end mirrors).

To make a quantitative analysis of the cavity spectrum and the features in Fig. 1b-d, we developed a perturbative solution of the Helmholtz equation to calculate the eigenmodes and eigenfrequencies of a symmetric optical cavity into which a dielectric slab is placed at an arbitrary location and tilt. As described elsewhere,[16] the empty-cavity eigenfrequencies are perturbed by an amount proportional to the eigenvalues of the matrix $\mathbf{V}$, where $V_{i,j} \propto \iiint \psi_i(x,y,z)\psi_j(x,y,z)\,dx\,dy\,dz$. Here ψ_k is the k^{th} unperturbed eigenmode of the cavity and the integral is taken over the volume of the membrane.

Applying this theory to the four cavity modes of interest (the singlet and triplet modes) quantitatively reproduces the large-scale ($\sim$GHz) sinusoidal shape of $\omega(x)$ seen in Fig. 1b if we assume $\mathrm{Re}[n] = 2.0$ and $t = 39$ nm (black lines). The discrepancy between the fitted and nominal values of t presumably reflects a combination of fabrication tolerances (~ 5 nm) and the limits of a first-order perturbation theory that includes only four eigenmodes. Nonetheless, the intermediate-scale ($\sim$10 MHz) features in Fig. 1c(i-ii), such as the lifting of the triplet's degeneracy, are also quantitatively reproduced (Fig. 1c(iii-iv)). Small-scale features such as avoided crossings agree with the model reasonably well and are discussed below.

2 Tunability of quadratic coupling

The second result of this article is that ω'' can be tuned over a wide range by moving the membrane along the $\tilde{x}$ axis. This tunability is important because in some situations it may be desirable to decrease ω'' in order to relax other experimental constraints. For example, if ω_s ($\propto 1/\omega''$) is small enough the membrane's motion may result in non-adiabatic transfer of light between the two cavity modes via Landau-Zener-Stückelberg-like transitions.[17]

The tunability of ω'' is illustrated in Fig. 2a-b, which each show six avoided crossings between the singlet and triplet modes. When the membrane is at the cavity waist (Fig. 2a) the upper gaps (triangles) are open and the lower gaps (squares) are closed. When the membrane is displaced 500 μm (Fig. 2b) from the waist, the two lower gaps open, the upper right gap opens further, and the upper left gap closes. The full dependence of ω_s on membrane position is shown in Fig. 2c.

The perturbative model (Fig. 2c inset) reproduces the linear dependence of $\omega_s(x)$ as well as the slope $\partial\omega_s/\partial x$ measured for each of the six gaps. The model differs from the data by a constant offset $\sim 3-4$ MHz for the middle and upper gaps (triangles and crosses in Fig. 2c), which we attribute to asymmetry in the cavity that is not included in the model. We find below (Fig. 3c) that it is possible to compensate for this intrinsic asymmetry by adjusting the *axis* of the membrane tilt.

3 Tunable coupling between motion and optical relaxation

In addition to creating large ω'', mixing between the cavity modes also causes the cavity loss rate κ to vary with x. Figure 3a(i) shows $\kappa(x)$ for the singlet and triplet modes (the corresponding detunings are shown in Fig. 3a(ii)). Far from the crossings each cavity mode has a different κ, reflecting the different overlap between each mode's transverse profile and the mirrors' inhomogeneities. At each avoided crossing the two modes swap their value of κ, leading to a large $\kappa' \equiv \partial\kappa/\partial x$. The dashed line in Fig. 3a indicates a crossing at which $\kappa' > 600$ kHz/nm.

Note that this data was taken with the membrane's tilt *axis* rotated by 45° to $(\tilde{y}+\tilde{z})/\sqrt{2}$, and the transverse eigenmodes have followed (inset camera images). The ability to rotate the transverse mode profiles provides some control over which portions of the mirrors the optical modes sample, and enables us to tune κ' *in situ*. In Fig. 3b we have rotated the membrane tilt axis back to $\tilde{z}$, with the result that the same crossing shows $\kappa' = -10$ kHz/nm. Significantly, the sign of κ' has changed, implying that at an intermediate tilt axis $\kappa' = 0$.

Gradients in κ can have several consequences. A linear variation of κ with x could preclude a QND measurement of n_m, so the ability to tune κ' to zero is appealing. Separately, it has been predicted that large values of κ' can be used to laser cool the membrane to its ground state even when the device is not in the resolved sideband regime.[18] However numerical estimates show that even with $\kappa' = 600$ kHz/nm, the usual optomechanical coupling[8,9] is more promising for laser-cooling the devices described here.

Variations in κ can also arise from optical absorption in the membrane. Previous measurements using non-stoichiometric SiN_x membranes found that variations in κ were proportional to the overlap of the intracavity standing wave and the membrane, and were consistent with $\mathrm{Im}(n) \approx 2 \times 10^{-4}$ for $\lambda = 1064$ nm.[15] Subsequent work found lower absorption in stoichiometric Si_3N_4 membranes, with $\mathrm{Im}(n) \lesssim 10^{-5}$ for $\lambda = 985$ nm.[19] Figure 3c shows κ for the TEM_{00} mode (using a Si_3N_4 membrane and $\lambda = 1064$ nm) as x is varied over a few λ. The small-scale ($\ll \lambda$) variations in $\kappa(x)$ are reproducible and periodic, and presumably arise from mixing with higher-order modes. To estimate the contribution to $\kappa(x)$ from absorption in the membrane (as opposed to mixing with higher-order modes), we extract the Fourier component of $\kappa(x)$ corresponding to the overlap between the membrane and the intracavity standing wave. This sets an upper limit of $\mathrm{Im}(n) \lesssim 1.5 \times 10^{-6}$ at $\lambda = 1064$ nm. The lower optical absorption observed here should enable the use of cavities with higher F while decreasing the quantum noise in the cavity and the heating of the membrane.

	F	$\omega''/2\pi$	$\omega_m/2\pi$	Q_m	m	
Quantum Jumps:	300,000	10 MHz/nm^2	100 kHz	1.2×10^7	50 pg	$\Sigma^{(0)} = 1.1$
Phonon Shot Noise:	50,000	0.9 MHz/nm^2	1 MHz	1.2×10^7	40 ng	$\mathcal{S} = 7.9$

Table 1: Comparison of parameters (cavity length L, finesse F, quadratic coupling ω'', membrane frequency ω_m, quality factor Q_m, and mass m) to observe energy quantization in a mechanical resonator for the two schemes. Both cases assume 5 μW of 1064-nm light incident on a cavity of length $L = 6.313$ cm in a ^{3}He cryostat, the membrane positioned within 0.5 pm of the avoided crossing, and the mechanical motion laser-cooled to $n_T < 0.2$ from a starting temperature $T = 300$ mK. For the phonon shot noise experiment, the estimate assumes the membrane is driven to 1 nm amplitude of motion.

4 Feasibility of observing mechanical energy quantization

To estimate the feasibility of observing energy quantization in the membrane, we first use the expressions derived elsewhere[13] for $\Sigma^{(0)}$, the signal-to-noise ratio for measurement of a single quantum jump. Assuming a single-port cavity,[20] we estimate $\Sigma^{(0)} = 1.1$ for a device with the parameters listed in the first row of Table 1. This scheme requires higher finesse and smaller values of m and ω_m (which could be realized by patterning the membrane into a free standing pad supported by narrow beams), as well as cryogenic pre-cooling to $T = 300$ mK. The key advances presented in this paper regarding the realization of this scheme are the demonstration of (i) sufficiently large ω'' and (ii) sufficiently low optical loss to meet these requirements.

The requirements for observing phonon shot noise in the membrane are described in Ref. [14]. The ratio between the phonon shot noise signal and the measurement imprecision for such a measurement is $\mathcal{S} = 8\bar{n}_m n_T \Sigma^{(0)}$, where $n_T = k_B T/\hbar\omega_m$. The parameters listed in the second row of Table 1 result in $\mathcal{S} = 7.9$. Significantly, these parameters correspond to the device demonstrated here; the value of $\omega''/2\pi = 0.9$ MHz/nm^2 corresponds to the lower avoided crossings resolved in Fig. 2b, and the amplitude of the membrane's motion ($x_0 = 1$ nm) is well below the onset of dynamical

bistability.[21] A quality factor $Q_m = 1.2 \times 10^7$ was demonstrated in similar membranes at $T = 300$ mK.[21]

5 Purely-quartic optomechanical coupling

The final point of this article is to demonstrate a new type of optomechanical nonlinearity: quartic (x^4) coupling. Figure 4a shows that when the membrane tilt is increased to ~ 1 mrad, $\omega(x)$ for the TEM_{20} mode undergoes a smooth transition from $\omega'' > 0$ (i) to $\omega'' < 0$ (iii); between these limits $\omega'' = 0$ (ii) and $\omega(x) \propto x^4$ to lowest order. A similar transition is visible in the faint background modes of Fig. 2a and Fig. 4b as a function of mode index.

This form of $\omega(x)$ can be used to realize an optomechanical coupling described (in the rotating wave approximation) by the Hamiltonian term $H^{(4)}_{\mathrm{coup}} = \hbar\omega^{(4)} x^4_{\mathrm{zpf}} n_\gamma n_m^2$, with $\omega^{(4)} \equiv \partial^4\omega^4/\partial x^4$, $x_{\mathrm{zpf}} = \sqrt{\hbar/2m\omega_m}$, and n_γ the intracavity photon number. This type of coupling can be used, for example, to prepare Schrödinger cat states in the membrane.[22,23]

While the quartic coupling in Fig. 4a is quite weak ($\omega^{(4)}/2\pi = 0.4$ Hz/nm^4), it may be possible to increase $\omega^{(4)}$ using avoided crossings. For example the interaction between the triplet and quintuplet modes (Fig. 4b) shows avoided crossings in which ω'' changes sign. In analogy with the tunability of ω'' demonstrated in Fig. 2c, we expect that careful arrangement of the membrane tilt and position will allow some of the crossings in Fig. 4b to be purely quartic with a substantially larger $\omega^{(4)}$.

6 Summary

In summary, we have demonstrated an optomechanical device in which the strength and the form of the optomechanical coupling can be tuned over a wide range *in situ*. We have demonstrated control over whether the optical cavity detuning is (to lowest order) linear, quadratic, or quartic in the displacement of a micromechanical membrane, and shown that the quadratic coupling is

three orders of magnitude stronger than previously demonstrated. This device also demonstrates extremely low optical loss, and an optical loss gradient that can be tuned to zero. These represent important advances in the ongoing effort to observe and manipulate quantum behavior in a solid mechanical oscillator.

In particular, the combination of low optical loss and strong quadratic coupling demonstrated here should enable the observation of the membrane's energy quantization without further improvements to the present device. This combination will also enable other functionalities related to quadratic coupling, including dispersive QND readout of the intracavity photon number, two-phonon laser cooling, conditional squeezing between the reflected light and the membrane's motion, and various types of passive optical squeezing.[15,24]

7 Methods

All measurements were performed at room temperature and pressure $< 10^{-5}$ Torr. The end mirrors were clamped to an invar spacer, and a mount equipped with three motorized actuators (for tilting and displacing the membrane) were mounted to this spacer. Two small piezoelectric elements provided finer positioning of the membrane along the cavity axis. Spectroscopy was performed by sweeping the frequency of a continuous wave Nd:YAG laser from low from low to high and stepping the membrane position with the piezo elements. The cavity's optical loss was measured via cavity ringdown.

8 Author information

Correspondence and requests for materials should be addressed to J.G.E.H.

9 Acknowledgments

We would like to thank H. Cao, A. Clerk, F. Marquardt, S. M. Girvin, A. Nunnenkamp, and D. Schuster. This work has been supported by grants from the NSF (#0855455 and #0653377) and AFOSR (#FA9550-90-1-0484). J.G.E.H. acknowledges support from the Alfred P. Sloan Foundation. This material is based upon work supported by DARPA Award No. N6601-09-1-2100 and W911NF-09-1-0015.

10 Author contributions

J.C.S. performed the measurements, developed the perturbation theory, and carried out the data analysis. C.Y., B.M.Z., A.M.J. assisted with each phase of the project. J.G.E.H. supervised each phase of the project.

References

[1] Kippenberg, T. J. & Vahala, K. J. Cavity opto-mechanics. *Opt. Express* **15**, 17172–17205 (2007).

[2] Schliesser, A., Arcizet, O., Riviere, R., Anetsberger, G. & Kippenberg, T. J. Resolved-sideband cooling and position measurement of a micromechanical oscillator close to the heisenberg uncertainty limit. *Nature Phys.* **5**, 509–514 (2009).

[3] Groblacher, S. *et al.* Demonstration of an ultracold micro-optomechanical oscillator in a cryogenic cavity. *Nature Phys.* **5**, 485–488 (2009).

[4] Park, Y.-S. & Wang, H. Resolved-sideband and cryogenic cooling of an optomechanical resonator. *Nature Phys.* **5**, 489–493 (2009).

[5] Arcizet, O. *et al.* High-sensitivity optical monitoring of a micromechanical resonator with a quantum-limited optomechanical sensor. *Phys. Rev. Lett.* **97**, 133601 (2006).

[6] Abbott, B. *et al.* Observation of a kilogram-scale oscillator near its quantum ground state. *New J. Phys.* **11**, 073032 (2009).

[7] Anetsberger, G. *et al.* Near-field cavity optomechanics with nanomechanical oscillators. *Nature Phys.* **5**, 909–914 (2009).

[8] Marquardt, F., Chen, J. P., Clerk, A. A. & Girvin, S. M. Quantum theory of cavity-assisted sideband cooling of mechanical motion. *Phys. Rev. Lett.* **99**, 093902 (2007).

[9] Rae, I. W., Nooshi, N., Zwerger, W. & Kippenberg, T. J. Theory of ground state cooling of a mechanical oscillator using dynamical backaction. *Phys. Rev. Lett.* **99**, 093901 (2007).

[10] Braginskii, V. B. & Vorontsov, Y. I. Quantum-mechanical limitations in macroscopic experiments and modern experimental technique. *Sov. Phys. Uspekhi* **17**, 644–650 (1975).

[11] Caves, C. M. Quantum-mechanical radiation-pressure fluctuations in an interferometer. *Phys. Rev. Lett.* **45**, 75–79 (1980).

[12] Tombesi, P. & Vitali, D. Physical realization of an environment with squeezed quantum fluctuations via quantum-nondemolition-mediated feedback. *Phys. Rev. A* **50**, 4253–4257 (1994).

[13] Thompson, J. D. *et al.* Strong dispersive coupling of a high-finesse cavity to a micromechanical membrane. *Nature* **452**, 72–75 (2008).

[14] Clerk, A., Marquardt, F. & Harris, J. Quantum measurement of phonon shot noise. *ArXiv e-prints* (2010). `1002.3140`.

[15] Jayich, A. M. *et al.* Dispersive optomechanics: a membrane inside a cavity. *New J. Phys.* **10**, 095008 (2008).

[16] Sankey, J. C., Jayich, A. M., Zwickl, B. M., Yang, C. & Harris, J. G. E. Improved "position squared" readout using degenerate cavity modes. *Proc. XXI Intl. Conf. Atomic Phys.* (2009).

[17] Heinrich, G., Harris, J. G. E. & Marquardt, F. Photon shuttle: Landau-zener-stückelberg dynamics in an optomechanical system. *Physical Review A* **81**, 011801 (2010).

[18] Elste, F., Girvin, S. M. & Clerk, A. A. Quantum noise interference and backaction cooling in cavity nanomechanics. *Phys. Rev. Lett.* **102**, 207209 (2009).

[19] Wilson, D. J., Regal, C. A., Papp, S. B. & Kimble, H. J. Cavity optomechanics with stoichiometric sin films. *Phys. Rev. Lett.* **103**, 207204 (2009).

[20] Miao, H., Danilishin, S., Corbitt, T. & Chen, Y. Standard quantum limit for probing mechanical energy quantization. *Phys. Rev. Lett.* **103**, 100402 (2009).

[21] Zwickl, B. M. *et al.* High quality mechanical and optical properties of commercial silicon nitride membranes. *Appl. Phys. Lett.* **92**, 103125 (2008).

[22] Yurke, B. & Stoler, D. Generating quantum mechanical superpositions of macroscopically distinguishable states via amplitude dispersion. *Phys. Rev. Lett.* **57**, 13–16 (1986).

[23] Jacobs, K. Engineering quantum states of a nanoresonator via a simple auxiliary system. *Phys. Rev. Lett.* **99**, 117203 (2007).

[24] Nunnenkamp, A., Borkje, K., Harris, J. G. E. & Girvin, S. M. Cooling and squeezing via quadratic optomechanical coupling. *ArXiv e-prints* (2010). `1004.2510`.

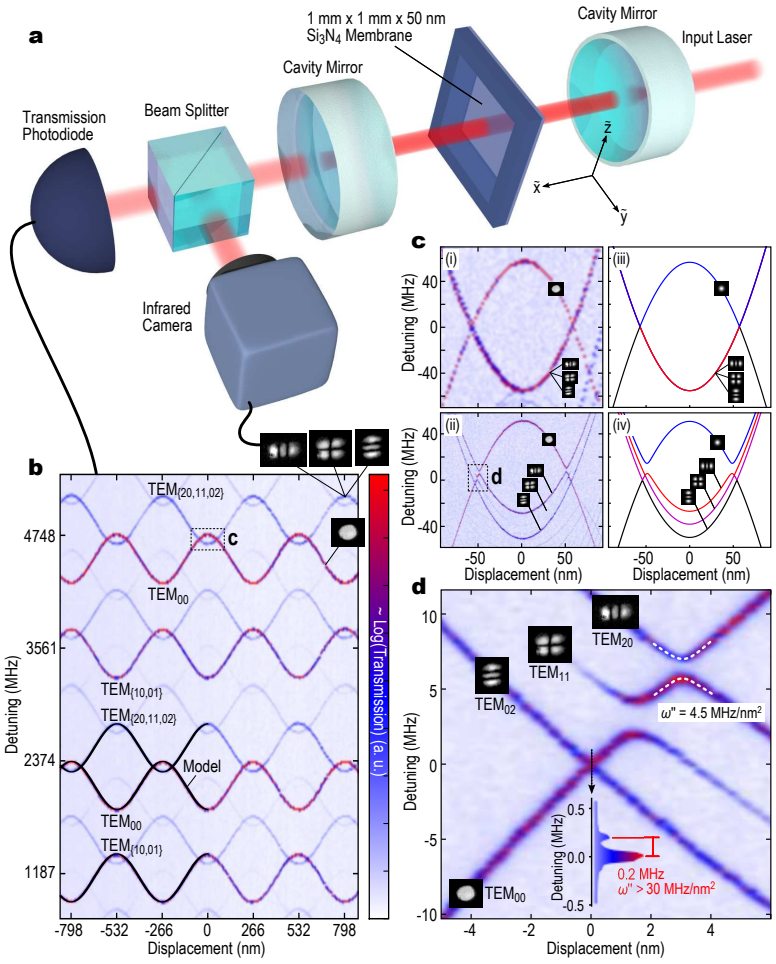

Figure 1: Avoided crossings in cavity spectra. **a** Schematic of our setup. **b** Cavity transmission as a function of laser detuning and membrane displacement. The membrane is positioned near the cavity waist, and the input laser is coupled to the lower-order transverse cavity modes. The transverse modes corresponding to the strongest transmission peaks are labeled. Images of each of these modes (captured with an infrared camera) are shown. Solid lines show model results. **c**(i,ii) Refined scans of the box labeled "c" in **a** with the membrane (i) aligned and (ii) tilted by 0.4 mrad. (iii) and (iv) show the corresponding predictions of the model. **d** Refined scan of the box labeled "d" in **c**(ii).

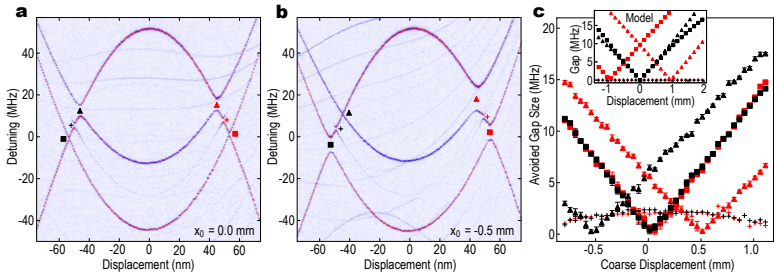

Figure 2: Tunability of avoided crossings for the membrane tilted 0.48 mrad about $\tilde{z}$. **a** Transmission spectrum for the membrane positioned near the cavity waist ($x = 0$ μm). **b** Transmission spectrum for the membrane displaced by -0.5 mm. **c** Magnitudes of the gaps labeled in **a** & **b** plotted as a function of the membrane's displacement. Error bars indicate the frequency resolution of the transmission spectra from which the gaps were estimated. (inset) Magnitudes of the same gaps calculated from the model described in the text.

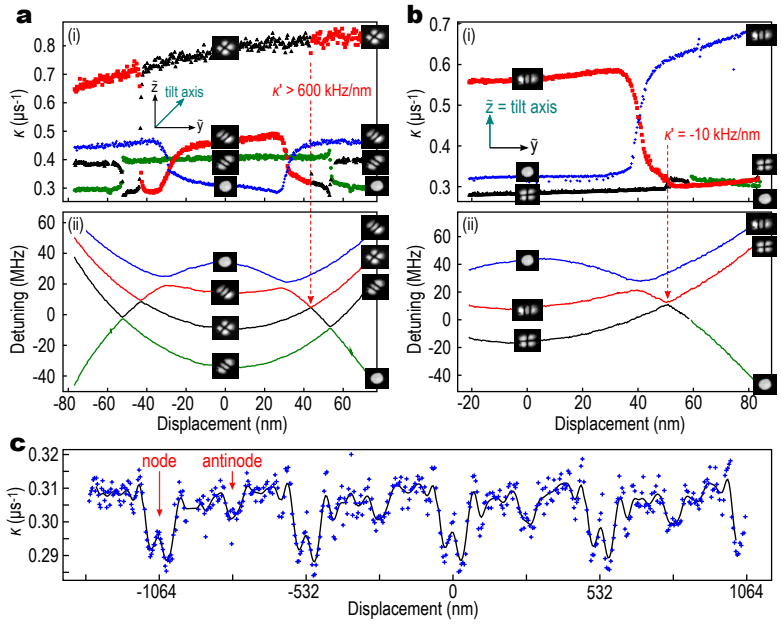

Figure 3: Optical relaxation gradients at avoided crossings. **a** Measurements of (i) cavity relaxation rate and (ii) detuning for each cavity mode versus position for the membrane tilted 0.66 mrad about the axis indicated in the figure. **b** Same but for the membrane tilted 0.61 mrad about a different axis (indicated in the figure). The dotted arrows highlight the crossing whose gradient κ' reverses sign. **c** Relaxation rate κ of the TEM_{00} mode as a function of membrane position. Symbols are data, the black solid line is a smoothed version of the data to show the $\lambda/2 = 532$ nm periodicity.

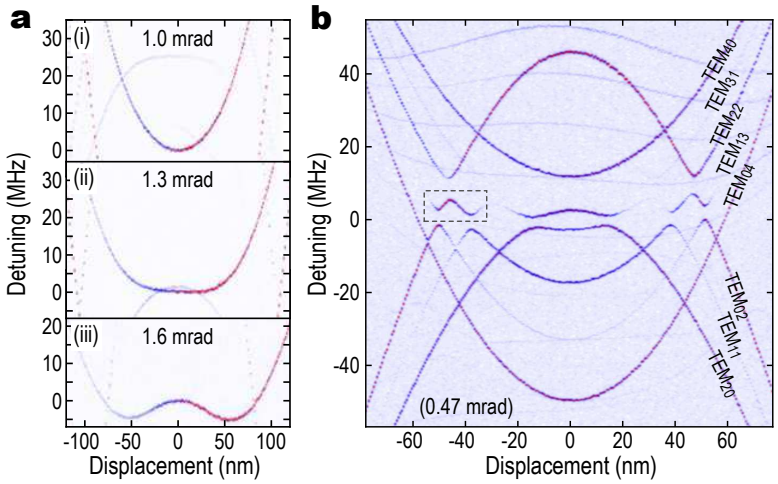

Figure 4: Quartic and double-well optomechanical coupling. **a** Transmission spectrum for the TEM_{20} mode with the membrane tilted to: (i) 1.0, (ii) 1.3, and (iii) 1.6 mrad, showing transition from (i) quadratic to (ii) quartic to (iii) double-well detunings. **b** Transmission of the cavity showing the avoided crossings between the $\mathrm{TEM}_{\{20,11,02\}}$ and $\mathrm{TEM}_{\{40,31,22,13,04\}}$ modes.

Cooling and squeezing via quadratic optomechanical coupling

A. Nunnenkamp, K. Børkje, J. G. E. Harris, and S. M. Girvin
Departments of Physics and Applied Physics, Yale University, New Haven, Connecticut 06520, USA
(Dated: April 21, 2010)

We explore the physics of optomechanical systems in which an optical cavity mode is coupled parametrically to the *square* of the position of a mechanical oscillator. We derive an effective master equation describing two-phonon cooling of the mechanical oscillator. We show that for high temperatures and weak coupling, the steady-state phonon number distribution is non-thermal (Gaussian) and that even for strong cooling the mean phonon number remains finite. Moreover, we demonstrate how to achieve mechanical squeezing by driving the cavity with two beams. Finally, we calculate the optical output and squeezing spectra. Implications for optomechanics experiments with the membrane-in-the-middle geometry or ultracold atoms in optical resonators are discussed.

PACS numbers: 37.30.+i, 42.50.Lc, 42.65.-k, 85.85.+j

Introduction. In optomechanical systems optical and mechanical degrees of freedom are coupled via radiation pressure, optical gradient, or photothermal forces. While work in this area was originally motivated by the goal of building sensitive detectors for gravitational waves [1, 2], the field has become an active area of research in its own right. Its main goal is to investigate quantum coherence in macroscopic solid-state devices both for quantum information purposes and gaining new insights into the quantum-to-classical transition [3, 4].

In most optomechanical experiments an optical cavity mode is parametrically coupled to the position of a mechanical oscillator. Consequently, many properties of this setup have been discussed, including red-sideband laser cooling in the resolved-sideband limit [5, 6], normal-mode splitting [7, 8], optical squeezing [9, 10], backaction-evading measurements [11–13], mechanical squeezing using either feedback [12, 14], squeezed light [15] or modulation of input power [16], and entanglement between light and a mechanical oscillator [17].

However, some optomechanical systems feature a quadratic optomechanical interaction, i.e. an optical cavity mode is coupled parametrically to the *square* of the position of a mechanical oscillator. One example is the membrane-in-the-middle geometry, in which the membrane is placed at a node or antinode of the cavity field [18–20]. A second system which can realize quadratic optomechanical coupling is a cloud of ultracold atoms loaded into an optical cavity, where the cloud's center-of-mass coordinate serves as the mechanical degree of freedom [21]. To date, the theoretical literature has focused on using the quadratic coupling to detect phonon Fock states [18, 19, 22–24], but otherwise the possible uses of this form of optomechanical coupling are largely unstudied.

In this paper we explore three features of quadratic optomechanical coupling: two-phonon cooling of the mechanical oscillator, squeezing of the mechanical oscillator, and squeezing of the optical output field. Using Fermi's Golden rule we first write down an effective master equation for the mechanical oscillator. In the classical limit of large phonon number, two-phonon cooling processes change the steady-state number distribution from exponential to Gaussian, a consequence of the nonlinear damping. In the quantum limit we find that ground-state cooling is not possible since two-phonon cooling processes preserve the phonon-number parity. We then demonstrate that the model maps onto a degenerate parametric oscillator if the cavity is driven by two laser beams whose frequencies are detuned to either side of the cavity resonance by an amount equal to the mechanical frequency. This opens up the possibility of mechanical squeezing. Finally, we calculate the optical output spectrum and find that this system is capable of producing considerable optical squeezing.

Hamiltonian. We start from the Hamiltonian (with $\hbar = 1$)

$$\hat{H} = \left(\omega_R + g\hat{x}^2\right)\left(\hat{a}^\dagger\hat{a} - \langle\hat{a}^\dagger\hat{a}\rangle\right) + \omega_M\hat{b}^\dagger\hat{b} + \hat{H}_\gamma + \hat{H}_\kappa \quad (1)$$

where ω_R is the cavity resonance frequency, g the quadratic optomechanical coupling, and $\hat{x} = x_{\rm ZPF}(\hat{b} + \hat{b}^\dagger)$ the position of the mechanical oscillator with zero-point fluctuations $x_{\rm ZPF} = (2m\omega_M)^{-1/2}$, frequency ω_M and mass m. $\hat{a}$ and $\hat{b}$ are annihilation operators obeying bosonic commutation relations. $\hat{H}_\gamma$ and $\hat{H}_\kappa$ describe the coupling to the mechanical and optical baths and the optical drive. We have subtracted the steady-state mean photon number $\langle\hat{a}^\dagger\hat{a}\rangle$ which renormalizes the frequency of the mechanical oscillator. The Hamiltonian (1) is relevant to systems with membrane-in-the-middle geometry [18], to ultracold atoms in optical resonators [21], and double-microdisk whispering-gallery mode resonators [30] when the first derivative of the cavity dispersion relation $\omega_{\rm cav}(x)$ vanishes, i.e. $\omega'_{\rm cav}(x_0) = 0$, so that $g = \omega''_{\rm cav}(x_0)/2$ is the leading order of the optomechanical coupling.

Expressing $\hat{a} = e^{-i\omega_L t}(\bar{a} + \hat{d})$ with the laser frequency ω_L, choosing $\bar{a}$ real, and neglecting $\hat{d}^\dagger\hat{d}$ with respect to $\bar{a}(\hat{d}^\dagger + \hat{d})$, we obtain the following quantum master equation

$$\dot{\varrho} = -i\left[\hat{H}_S, \varrho\right] + \kappa\mathcal{D}[\hat{d}]\varrho + \gamma(1+n_{\rm th})\mathcal{D}[\hat{b}]\varrho + \gamma n_{\rm th}\mathcal{D}[\hat{b}^\dagger]\varrho \quad (2)$$

with the system Hamiltonian

$$\hat{H}_S = -\Delta\hat{d}^\dagger\hat{d} + \omega_M\hat{b}^\dagger\hat{b} + \bar{g}(\hat{b} + \hat{b}^\dagger)^2(\hat{d}^\dagger + \hat{d}) \quad (3)$$

where $\Delta = \omega_L - \omega_R$ is the detuning, $\bar{g} = g\bar{a}x_{\rm ZPF}^2$ the coupling, κ and γ the cavity and mechanical damping rates, and $n_{\rm th}$ the thermal phonon number. We assume that the optical bath is at zero temperature. $\mathcal{D}[\hat{o}]\varrho = \hat{o}\varrho\hat{o}^\dagger - (\hat{o}^\dagger\hat{o}\varrho + \varrho\hat{o}^\dagger\hat{o})/2$ denotes the standard dissipator in Lindblad form.

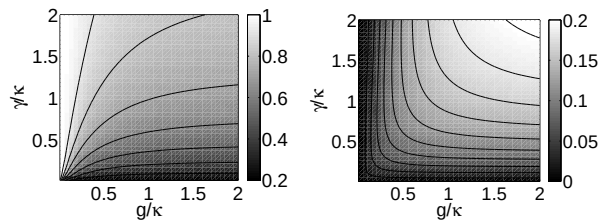

FIG. 1: Steady-state mean phonon $\langle \hat{b}^\dagger \hat{b} \rangle$ (left) and photon number $\langle \hat{d}^\dagger \hat{d} \rangle$ (right) as a function of the coupling strength g/κ and thermal coupling γ/κ for thermal phonon number $n_{\rm th} = 1$, obtained from the numerical solution of the full quantum master equation (2).

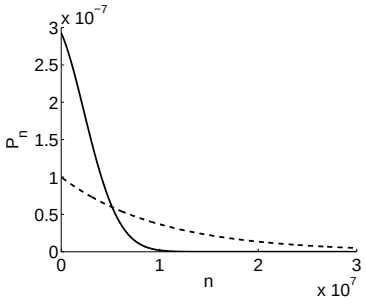

FIG. 2: Steady-state phonon number distribution P_n for thermal phonon number $n_{\rm th} = 10^7$ and for $\Gamma_\downarrow = 0$ (dashed) and $\Gamma_\downarrow/\gamma = 4 \cdot 10^{-7}$ (solid), respectively.

Numerical simulations of the full quantum master equation. If the cavity is driven on the red two-phonon resonance, i.e. $\Delta = -2\omega_M$, in the good-cavity limit, i.e. $\kappa \ll \omega_M$, we expect two-phonon cooling processes to be important. Concentrating on the resonant terms, i.e. $\hat{H}_S = \bar{g}(\hat{b}^\dagger \hat{b}^\dagger \hat{d} + h.c.)$, we solve the full quantum master equation (2) numerically for small thermal phonon numbers $n_{\rm th}$. We find three different regimes: (i) for $\gamma n_{\rm th} \ll \kappa$ the mechanical oscillator is cooled due to the coupling to the zero-temperature bath of the optical field [25], (ii) for $\gamma n_{\rm th} \gg \kappa$ the optical field is heated by the coupling to the mechanical oscillator, and (iii) for $\gamma n_{\rm th} \approx \kappa$ both effects are important and the density matrix has non-zero off-diagonal elements so that e.g. the correlator $|\langle \hat{d}^\dagger \hat{b} \hat{b} \rangle|$ is non-zero. As an example we plot in Fig. 1 the steady-state mean phonon number $\langle \hat{b}^\dagger \hat{b} \rangle$ and the mean number of photons due to the coupling to the membrane $\langle \hat{d}^\dagger \hat{d} \rangle$ as a function of the coupling strength $\bar{g}/\kappa$ and thermal coupling γ/κ for thermal phonon number $n_{\rm th} = 1$.

Effective master equation describing two-phonon cooling. For $\gamma n_{\rm th} \ll \kappa$ and weak coupling, i.e. $\bar{g} \ll \kappa$, we can employ a quantum noise approach [25], i.e. we calculate two-phonon cooling and amplification rates using Fermi's Golden rule. Concentrating on the diagonal terms of the density matrix $\varrho_{nn} = P_n$, we write down a set of rate equations

$$\begin{aligned} \dot{P}_n = & -\gamma \left(n_{\rm th}(n+1) + (n_{\rm th}+1)n \right) P_n \\ & + \gamma n_{\rm th} n P_{n-1} + \gamma (n_{\rm th}+1)(n+1) P_{n+1} \\ & - \left(\Gamma_\downarrow n(n-1) + \Gamma_\uparrow (n+2)(n+1) \right) P_n \\ & + \Gamma_\downarrow (n+2)(n+1) P_{n+2} + \Gamma_\uparrow n(n-1) P_{n-2}. \end{aligned} \quad (4)$$

The terms in the first two lines are due the coupling of the mechanical oscillator to its thermal bath with rate γ and thermal phonon number $n_{\rm th}$. The terms in the last two lines are due to two-phonon processes whose rates are governed by $\Gamma_{\downarrow/\uparrow} = g^2 x_{\rm ZPF}^4 S_{nn}(\pm 2\omega_M)$ where $S_{nn}(\omega) = \kappa |\bar{a}|^2 |\chi_R(\omega)|^2$ is the photon number spectral density and $\chi_R(\omega) = [\kappa/2 - i(\omega + \Delta)]^{-1}$ the cavity response function. We note that nonlinear damping of a mechanical oscillator was studied in Ref. [26].

The infinite set of rate equations (4) can be replaced by a single differential equation for the generating function $F(z,t) = \sum_{n=0}^{\infty} P_n(t) z^n$. For vanishing two-phonon amplification $\Gamma_\uparrow = 0$ the steady-state equation can be solved exactly in terms of the confluent hypergeometric function [27].

We point out that it is an advantage of quadratic cooling that it enables cooling when the membrane or atoms are placed at a node of the cavity field. In this situation the system is most insensitive to absorption from the membrane or atoms as well as to bistability from radiation pressure.

Two-phonon cooling in the classical limit. For large thermal phonon number $n_{\rm th} \gg 1$ and weak two-phonon cooling $\gamma n_{\rm th} \gg \Gamma_\downarrow$ we can replace the quantum operators $\hat{b}$ and $\hat{d}$ in their Heisenberg equations of motion by complex amplitudes $\beta = \langle \hat{b} \rangle$ and $\alpha = \langle \hat{d} \rangle$ and obtain two coupled classical Langevin equations $\dot{\beta} = -\gamma\beta/2 - 2i\bar{g}\beta^*\alpha + \xi$ and $\dot{\alpha} = -\kappa\alpha/2 - i\bar{g}\beta^2$, where the thermal noise is characterized by $\langle \xi(t)\xi^*(t') \rangle = \gamma n_{\rm th} \delta(t-t')$. Adiabatically eliminating the optical field we obtain an equation of motion with a nonlinear damping term $\dot{\beta} = -\gamma\beta/2 - 4\bar{g}^2|\beta|^2\beta/\kappa + \xi$. Solving the corresponding Fokker-Planck equation we obtain the phonon number distribution

$$P_n \propto \exp\left(-\frac{n}{n_{\rm th}}\right) \exp\left(-\frac{\Gamma_\downarrow n^2}{\gamma n_{\rm th}}\right). \quad (5)$$

The distribution changes from an exponential for $\gamma/\Gamma_\downarrow \gg n_{\rm th}$ to a Gaussian for $\gamma/\Gamma_\downarrow \ll n_{\rm th}$. In the latter limit the mean phonon number is given by $\langle n \rangle = \sqrt{\gamma n_{\rm th} \kappa/\pi\bar{g}^2}$. The expression in Eq. (5) agrees with the high-temperature limit of the exact solution to the rate equations [27]. We conclude that the change in the steady-state phonon number distribution is a purely classical effect due to nonlinear damping.

The quadratic coupling in current membrane-in-the-middle experiments is very small $\bar{g}/\kappa = 10^{-5}$. Nonetheless, it leads to sizable effects if the thermal phonon number $n_{\rm th}$ is large. In Fig. 2 we plot the steady-state phonon number distribution for a thermal phonon number $n_{\rm th} = 10^7$ both in the absence $\Gamma_\downarrow = 0$ and presence $\Gamma_\downarrow/\gamma = 4 \cdot 10^{-7}$ of two-phonon cooling. We find the Planck distribution with mean $n_{\rm th} = 10^7$ becomes a nearly-Gaussian distribution with mean $n_{\rm th} = 2.8 \cdot 10^6$.

Two-phonon cooling in the quantum limit. Experiments with ultracold atoms are in the opposite limit with small thermal heating rate $\gamma n_{\rm th}$ and strong optomechanical coupling $\bar{g}$. Solving the rate equations (4) in the limit of strong optical damping, i.e. $\Gamma_\downarrow \gg \gamma n_{\rm th}$, we obtain the phonon number distribution $P_0/P_1 = 3 + 1/n_{\rm th}$ with all other $P_n = 0$ and the

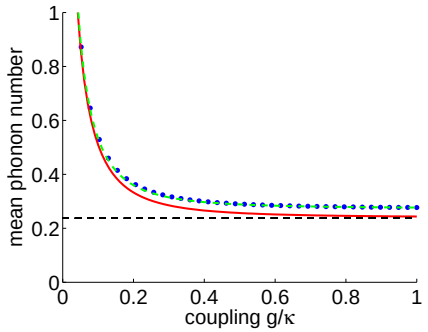

FIG. 3: (Color online) Mean phonon number $\langle \hat{b}^\dagger \hat{b} \rangle$ as a function of coupling $\bar{g}/\kappa$ obtained from the quantum master equation (blue dots) and the classical rate equations without (red solid) and with strong-coupling correction (green dashed). The black dashed line indicates the minimal phonon number $\bar{n}_M^0$ given by Eq. (6) for $n_{\rm th} = 5$.

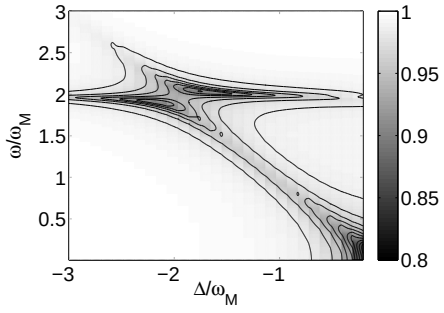

FIG. 4: Optimal squeezing spectrum of the cavity output field $S_{\rm opt}^{\rm out}(\omega)$ as a function of detuning Δ. The parameters are $\omega_m/\kappa = 5$, $\bar{g}/\kappa = 0.5$, $\gamma/\kappa = 0.1$ and $n_{\rm th} = 0$.

minimal mean phonon number

$$\bar{n}_M^0 = \frac{1}{4 + \frac{1}{n_{\rm th}}}. \tag{6}$$

The fact that strong cooling leaves both ground and first excited state occupied is a consequence of the fact that two-phonon cooling processes preserve the phonon-number parity.

In Fig. 3 we plot the steady-state phonon number $\langle \hat{b}^\dagger \hat{b} \rangle$ as a function of coupling $\bar{g}$ obtained from the full quantum master equation (2) and the rate equations (4). The two results show excellent agreement at weak coupling $\bar{g} \ll \kappa$. As $4\bar{g}^2/\kappa$ becomes comparable to κ, the Fermi's Golden rule expression for two-phonon cooling breaks down and the predictions of the full master equation (2) and the weak-coupling rate equations (4) will in general be different. In the limit where only the Fock states with phonon number $n \leq 3$ are important, we adiabatically eliminate the off-diagonal terms in the quantum master equation (2) and find that the strong-coupling two-phonon cooling rates are given by

$$\Gamma_{n,n-2}^{\downarrow} = \frac{4\bar{g}^2 n(n-1)\kappa}{\kappa^2 + 4\bar{g}^2 n(n-1)}. \tag{7}$$

In the weak-coupling limit $\bar{g} \ll \kappa$ this expression simplifies to our previous result $4\bar{g}^2 n(n-1)/\kappa$. In the limit of strong coupling $\bar{g} \gg \kappa$, the two-phonon cooling rate $\Gamma_{n,n-2}^{\downarrow}$ remains finite and cannot exceed the cavity damping rate κ. This leads to a minimum phonon number which is larger than the one predicted from the weak-coupling theory. In Fig. 3 we plot the steady-state mean phonon number obtained from the modified rate equations and find excellent agreement with the exact solution to the full quantum master equation (2).

We note that for quadratic coupling in the good-cavity limit, the phonon number distribution P_n can be measured by monitoring the phase shift of the reflected light [18, 19, 22].

Squeezing the mechanical oscillator. Driving the cavity at both $\omega_R \pm \omega_M$ with equal strength, the classical part of the cavity field oscillates in time $\bar{a} = A\cos\omega_M t$. In the case of linear optomechanical coupling this enables a backaction-evading measurement of one quadrature of the mechanical oscillator [11–13], but does not itself produce squeezing apart from the one which is conditioned on the measurement outcome. When we instead consider the same drive applied to a system with quadratic coupling, moving to an interaction picture with respect to $\hat{H}_0 = \omega_R \hat{a}^\dagger \hat{a} + \omega_M \hat{b}^\dagger \hat{b}$ and keeping only non-rotating terms of the quadratic coupling, we obtain the Hamiltonian of the degenerate parametric oscillator, i.e. $\hat{H}_{\rm DPO} = \frac{\chi}{2}(\hat{b}^2 + (\hat{b}^\dagger)^2)$ with $\chi = g x_{\rm ZPF}^2 A/2$.

Solving the linear quantum Langevin equations we see that the steady-state fluctuations in the quadrature $\hat{X} = (\hat{b}e^{i\omega_M t} + H.c.)/\sqrt{2}$ of the mechanical oscillator are squeezed below the thermal level, $\langle \hat{X}^2 \rangle = \frac{n_{\rm th}+1/2}{1+2\chi/\gamma}$, depending on the ratio χ/γ. At threshold $\chi = \gamma/2$, i.e. before the parametric oscillator becomes unstable, it is maximal and equal to -3dB [28]. Although the parameters of current membrane-in-the-middle setups show small coupling $\bar{g} \ll \kappa$ and large thermal phonon number $n_{\rm th} \gg 1$, we emphasize that the ratio χ/γ which is of importance here can still be comparable to unity and lead to significant noise squashing.

The mechanical squeezing can be detected by coupling the position of the mechanical oscillator parametrically to a second optical mode. This scenario has been studied in Ref. [14].

Output spectrum. Let us now return to the full model (3). Up to second order in the coupling $\bar{g}$, the cavity output spectrum which is defined as $S_{dd}^{\rm out}(\omega) = \int dt\, e^{i\omega t} \langle \hat{d}_{\rm out}(t) \hat{d}_{\rm out}^\dagger(0) \rangle$ with $\hat{d}_{\rm out} = \hat{d}_{\rm in} + \sqrt{\kappa}\hat{d}$ and $\langle \hat{d}_{\rm in}(t) \hat{d}_{\rm in}^\dagger(t) \rangle = \delta(t-t')$ is given by $S_{dd}^{\rm out}(\omega) = 4\kappa\bar{g}^2 |\chi_R[-\omega]|^2 S_{x^2x^2}(\omega)$ where

$$S_{x^2x^2}(\omega) = \frac{\gamma(n_{\rm th}+1)^2}{\gamma^2 + (\omega - 2\omega_M)^2} + \frac{\gamma n_{\rm th}^2}{\gamma^2 + (\omega + 2\omega_M)^2} + \frac{2\gamma n_{\rm th}(n_{\rm th}+1)}{\gamma^2 + \omega^2}. \tag{8}$$

We see the output spectrum $S_{dd}^{\rm out}(\omega)$ has sidebands at $\omega = \pm 2\omega_m$ and $\omega = 0$ as expected for quadratic coupling.

Optical squeezing spectrum. One application of optomechanical devices which has been widely advocated [9, 10] is to use the nonlinear coupling between light and mirror to

squeeze the incoming coherent light beam, i.e. reduce one of its quadratures below the shot-noise level at certain frequencies. The quantity which characterizes this noise reduction is the optical squeezing spectrum $S_\theta^{\rm out}(\omega)$ given by [29]

$$S_\theta^{\rm out}(\omega) = 1 + \int_{-\infty}^{\infty} dt\, e^{i\omega t} \langle : \hat{X}_\theta^{\rm out}(t), \hat{X}_\theta^{\rm out}(0) : \rangle$$
$$= 1 + \kappa \int_{-\infty}^{\infty} dt\, e^{i\omega t} \mathcal{T} \left[\langle : \hat{X}_\theta(t), \hat{X}_\theta(0) : \rangle \right] \quad (9)$$

where $\hat{X}_\theta^{\rm out} = (\hat{d}_{\rm out}^\dagger e^{i\theta} + H.c.)/2$, $\langle A, B\rangle = \langle AB\rangle - \langle A\rangle\langle B\rangle$, the colons indicate normal ordering and $\mathcal{T}$ is the time-ordering operator [29]. The former expression is useful for calculations in input-output theory and the latter for master equation simulations evoking the quantum regression theorem.

In Fig. 4 we plot the optimal squeezing spectrum of the cavity output field $S_{\rm opt}^{\rm out}(\omega) = \min_\theta S_\theta^{\rm out}(\omega)$ as a function of detuning Δ. In the good-cavity limit at zero temperature we find considerable squeezing at $\omega = 0$ and $\omega = 2\omega_M$ for $\Delta = 0$ and $\Delta = -2\omega_M$, respectively. We choose parameters $\omega_m/\kappa = 5$, $\bar{g}/\kappa = 0.5$, $\gamma/\kappa = 0.1$ and $n_{\rm th} = 0$, relevant to experiments with ultracold atoms in optical resonators.

To gain insight beyond numerics we obtain the squeezing spectrum perturbatively up to second order in the coupling $\bar{g}$

$$S_{\rm opt}^{\rm out}(\omega) = 1 + S_{dd}^{\rm out}(\omega) + S_{dd}^{\rm out}(-\omega)$$
$$- 8\bar{g}^2\kappa \Big| \chi_R(\omega)\chi_R(-\omega) S_{x^2x^2}(\omega)$$
$$- \left(n_{\rm th} + \frac{1}{2}\right) \chi_R^*(\omega)\chi_R(-\omega) \left(\kappa\chi_R(\omega) - 1\right)$$
$$\times \left[\frac{1}{\gamma + i(\omega - 2\omega_M)} - \frac{1}{\gamma + i(\omega + 2\omega_M)} \right] \Big| . \quad (10)$$

As in the case of linear optomechanical coupling [9, 10], we find two regimes of strong squeezing: for small detuning and small frequencies as well as for detuning and frequencies close to twice the mechanical frequency. However, thermal fluctuations are more destructive for squeezing effects with quadratic optomechanical coupling due to the quadratic scaling with the thermal phonon number $n_{\rm th}$ and due to the fact that the spectrum $S_{x^2x^2}(\omega)$ has weight at zero frequency.

Conclusions. We have explored the physics of nonlinear optomechanical systems where an optical cavity mode couples quadratically rather than linearly to the position of a mechanical oscillator. For optomechanical experiments with the membrane-in-the-middle geometry, we predict a qualitative change in the phonon number distribution and mechanical noise squashing. For ultracold atoms in optical resonators, we found the quantum limit for two-phonon cooling and sizable mechanical and optical squeezing.

Acknowledgements. AN thanks E. Ginossar for useful discussions. We acknowledge support from NSF under Grant No. 0603369 (AN and SMG), 0653377 (AN, JGEH, and SMG) and 0855455 (JGEH), from the Research Council of Norway under Grant No. 191576/V30 (KB), and from AFOSR under Grant No. FA9550-90-1-0484 (JGEH). This material is based upon work supported by DARPA under award No. N6601-09-1-2100 and W911NF-09-1-0015.

[1] C. M. Caves, K. S. Thorne, R. W. P. Drever, V. D. Sandberg, and M. Zimmermann, Rev. Mod. Phys. **52**, 341 (1980).
[2] B. C. Barish and R. Weiss, Physics Today **52**, 44 (1999).
[3] T. J. Kippenberg and K. J. Vahala, Science **321**, 1172 (2008).
[4] F. Marquardt and S. M. Girvin, Physics **2**, 40 (2009).
[5] I. Wilson-Rae, N. Nooshi, W. Zwerger, and T. J. Kippenberg, Phys. Rev. Lett. **99**, 093901 (2007).
[6] F. Marquardt, J. P. Chen, A. A. Clerk, and S. M. Girvin, Phys. Rev. Lett. **99**, 093902 (2007).
[7] J. M. Dobrindt, I. Wilson-Rae, and T. J. Kippenberg, Phys. Rev. Lett. **101**, 263602 (2008).
[8] S. Gröblacher, K. Hammerer, M. R. Vanner, and M. Aspelmeyer, Nature (London) **460**, 724 (2009).
[9] S. Mancini and P. Tombesi, Phys. Rev. A **49**, 4055 (1994).
[10] C. Fabre, M. Pinard, S. Bourzeix, A. Heidmann, E. Giacobino, and S. Reynaud, Phys. Rev. A **49**, 1337 (1994).
[11] V. B. Braginsky, Y. I. Vorontsov, and K. S. Thorne, Science **209**, 547 (1980).
[12] A. A. Clerk, F. Marquardt, and K. Jacobs, New J. Phys. **10**, 095010 (2008).
[13] J. B. Hertzberg, T. Rocheleau, T. Ndukum, M. Savva, A. A. Clerk, and K. C. Schwab, Nat. Phys. **6**, 213 (2010).
[14] M. J. Woolley, A. C. Doherty, G. J. Milburn, and K. C. Schwab, Phys. Rev. A **78**, 062303 (2008).
[15] K. Jähne, C. Genes, K. Hammerer, M. Wallquist, E. S. Polzik, and P. Zoller, Phys. Rev. A **79**, 063819 (2009).
[16] A. Mari and J. Eisert, Phys. Rev. Lett. **103**, 213603 (2009).
[17] D. Vitali, S. Gigan, A. Ferreira, H. R. Böhm, P. Tombesi, A. Guerreiro, V. Vedral, A. Zeilinger, and M. Aspelmeyer, Phys. Rev. Lett. **98**, 030405 (2007).
[18] J. D. Thompson, B. M. Zwickl, A. M. Jayich, F. Marquardt, S. M. Girvin, and J. G. E. Harris, Nature (London) **452**, 72 (2008).
[19] A. M. Jayich, J. C. Sankey, B. M. Zwickl, C. Yang, J. D. Thompson, S. M. Girvin, A. A. Clerk, F. Marquardt, and J. G. E. Harris, New J. Phys. **10**, 095008 (2008).
[20] J. C. Sankey, C. Yang, B. M. Zwickl, A. M. Jayich, and J. G. E. Harris, arXiv:1002.4158.
[21] K. W. Murch, K. L. Moore, S. Gupta, and D. M. Stamper-Kurn, Nat. Phys. **4**, 561 (2008).
[22] F. Helmer, M. Mariantoni, E. Solano, and F. Marquardt, Phys. Rev. A **79**, 052115 (2009).
[23] H. Miao, S. Danilishin, T. Corbitt, and Y. Chen, Phys. Rev. Lett. **103**, 100402 (2009).
[24] A. Clerk, F. Marquardt, and J. Harris, arXiv:1002.3140.
[25] A. A. Clerk, M. H. Devoret, S. M. Girvin, F. Marquardt, and R. Schoelkopf, Rev. Mod. Phys. **82**, 1155 (2010).
[26] M. Dykman and M. Krivoglaz, Phys. Stat. Sol. (b) **68**, 111 (1975).
[27] V. V. Dodonov and S. S. Mizrahi, J. Phys. A: Math. Gen. **30**, 5657 (1997).
[28] G. Milburn and D. F. Walls, Opt. Comm. **39**, 401 (1981).
[29] D. F. Walls and G. J. Milburn, *Quantum Optics* (Springer, 2008).
[30] O. Painter, private communication.